BIOCHEMISTRY
including biophysical chemistry & molecular biology
Article

Biochemistry **2010,** *49,* 6705–6714 6705
DOI: 10.1021/bi100486s

Phosphomimetic Substitution of Cytochrome *c* Tyrosine 48 Decreases Respiration and Binding to Cardiolipin and Abolishes Ability to Trigger Downstream Caspase Activation†

Petr Pecina,[‡] Grigory G. Borisenko,[§,∥] Natalia A. Belikova,[§] Yulia Y. Tyurina,[§] Alena Pecinova,[‡] Icksoo Lee,[‡] Alejandro K. Samhan-Arias,[§] Karin Przyklenk,[⊥] Valerian E. Kagan,[§] and Maik Hüttemann*[,‡]

[‡]*Center for Molecular Medicine and Genetics, and* [⊥]*Cardiovascular Research Institute, Department of Physiology, Wayne State University School of Medicine, Detroit, Michigan 48201,* [§]*Center for Free Radical and Antioxidant Health and Department of Environmental and Occupational Health, University of Pittsburgh, Pittsburgh, Pennsylvania 15219, and* [∥]*Research Institute of Physico-Chemical Medicine, Moscow, Russian Federation*

Received April 1, 2010; Revised Manuscript Received June 14, 2010

ABSTRACT: Mammalian cytochrome *c* (Cyt*c*) transfers electrons from the bc_1 complex to cytochrome *c* oxidase (CcO) as part of the mitochondrial electron transport chain, and it also participates in type II apoptosis. Our recent discovery of two tyrosine phosphorylation sites in Cyt*c*, Tyr97 in bovine heart and Tyr48 in bovine liver, indicates that Cyt*c* functions are regulated through cell signaling. To characterize the role of Cyt*c* tyrosine phosphorylation in detail using an independent approach, we here overexpressed and purified a Tyr48Glu mutant Cyt*c*, mimicking the *in vivo* Tyr48 phosphorylation found in cow liver, along with wild-type and Tyr48Phe variants as controls. The midpoint redox potential of the phosphomimetic mutant was decreased by 45 mV compared to control (192 vs 237 mV). Similar to Tyr48 *in vivo* phosphorylated Cyt*c*, direct kinetic analysis of the Cyt*c* reaction with isolated CcO revealed decreased V_{max} for the Tyr48Glu mutant by 30% compared to wild type or the Tyr48Phe variants. Moreover, the phosphomimetic substitution resulted in major changes of Cyt*c* functions related to apoptosis. The binding affinity of Tyr48Glu Cyt*c* to cardiolipin was decreased by about 30% compared to wild type or the Tyr48Phe variants, and Cyt*c* peroxidase activity of the Tyr48Glu mutant was cardiolipin-inducible only at high cardiolipin concentration, unlike controls. Importantly, the Tyr48Glu Cyt*c* failed to induce any detectable downstream activation of caspase-3. Our data suggest that *in vivo* Tyr48 phosphorylation might serve as an antiapoptotic switch and highlight the strategic position and role of the conserved Cyt*c* residue Tyr48 in regulating multiple functions of Cyt*c*.

Cytochrome *c* (Cyt*c*)[1] is a 12 kDa globular protein with a covalently attached heme group. It is located in the mitochondrial intermembrane space where it functions as a mobile electron carrier between complexes III and IV of the electron transport chain (ETC). Interaction with both complexes is mediated by a cluster of lysine residues on the protein surface, making Cyt*c* one of the most positively charged proteins, with a p*I* of 9.6. The role of Cyt*c* in mitochondrial ATP production is essential, as Cyt*c* knockout mice die around midgestation (*1*), when metabolism switches from the glycolytic pathway to aerobic energy production (*2*). During the last two decades it was revealed that Cyt*c* exerts additional functions beyond its classical role in bioenergetics. Aside from being an indispensable enzyme for fueling cellular life as part of the ETC, it can also be a key player for the cell's eventual downfall via type II apoptosis. In the latter case, triggered by proapoptotic signals, Cyt*c* is released from the mitochondria into the cytosol (*3*, *4*), where it binds to Apaf-1, which initiates the assembly of the apoptosome and the downstream activation of caspases (*5*). Interestingly, Cyt*c* is a major regulator of its own release from the mitochondria. Proapoptotic signals lead to excessive availability of the mitochondrial phospholipid cardiolipin that avidly binds to Cyt*c*. This interaction, causing partial unfolding of the enzyme and weakening of the coordinate bond between heme iron and Met80, turns the enzyme "wild", unleashing its peroxidase activity which is normally tamed by hexacoordinate binding of the heme iron (*6*). Subsequent peroxidation of cardiolipin as well as other lipids compromises the integrity of mitochondrial membranes, which precedes the release of Cyt*c* in the apoptotic sequence of events. Inside mitochondria, Cyt*c* is involved in yet other redox reactions. When detached from the membrane it can be reduced by superoxide, suggesting its role as a ROS detoxifying enzyme (*7*). $p66^{Shc}$, a protein implicated in life span regulation, was shown to produce H_2O_2 after being reduced by Cyt*c* in mitochondria (*8*).

Considering the multiple roles of Cyt*c*, one would expect that the enzyme must be tightly regulated. Aside from the long recognized allosteric regulation by ATP (*9*), Cyt*c* was not recognized as target for cellular signaling pathways until recently, when our group discovered phosphorylation of Tyr97 in Cyt*c* isolated from bovine heart (*10*). The phosphorylated enzyme displayed a 695 → 687 nm shift of the weak Met80 heme iron ligand absorption bond and had an increased K_M in reaction with cytochrome *c* oxidase (CcO) (*10*). Another phosphorylation on Tyr48 was later found in bovine liver Cyt*c*, resulting in about

†The financial support of the Center for Molecular Medicine and Genetics and the Cardiovascular Research Institute Isis Initiative, Wayne State University School of Medicine, Detroit, MI, is gratefully acknowledged.

*To whom correspondence should be addressed. Fax: (313) 577-5218. Telephone: (313) 577-9150. E-mail: mhuttema@med.wayne.edu.

[1]Abbreviations: au, arbitrary units; CcO, cytochrome *c* oxidase; CL, cardiolipin; Cyt*c*, cytochrome *c*; ESI-LC-MS, electrospray ionization−liquid chromatography−mass spectrometry; ETC, electron transport chain; PC, 1,2-dioleoyl-*sn*-glycero-3-phosphocholine; TLCL, tetralinoleylcardiolipin.

Published on Web 06/29/2010

50% reduction of V_{max} of the oxidation rate by CcO (*11*). The two mapped phosphoepitopes have been among the first tyrosine phosphorylation sites discovered in the mitochondrial proteome (*12*, *13*). The corresponding kinase(s) and phosphatase(s), however, remain elusive.

Cyt*c* isolation from tissues yields mixed preparations of phosphorylated and dephosphorylated protein, complicating a detailed biochemical comparison of the two species. In the present study, therefore, we used a prokaryotic overexpression system to obtain three versions of rodent Cyt*c*: wild type, phosphomimetic mutant Tyr48Glu, and Tyr48Phe as an additional control. We demonstrate that the phosphomimetic mutation results in a 50 mV drop of the Cyt*c* redox potential, decreased V_{max} of reaction with CcO, decreased binding affinity to cardiolipin, and alteration of its peroxidase activity. Importantly, Tyr48Glu mutant was incapable of inducing caspase activity *in vitro*, suggesting an antiapoptotic role for Tyr48 phosphorylation.

MATERIALS AND METHODS

Overexpression of Cytochrome c Wild Type and Mutants in the Prokaryotic System. All chemicals were purchased from Sigma (St. Louis, MO) unless stated otherwise. Mouse and rat somatic Cyt*c* have identical protein sequences and are referred to as rodent Cyt*c*. The pLW01 overexpression vector was used to generate rodent Cyt*c* constructs for overexpression in bacteria (*14*). This vector is specifically designed for Cyt*c* overexpression and also contains the cDNA encoding heme lyase (*CYC3*), which is not present in bacteria but necessary for covalent attachment of the heme group to the Cyt*c* apoenzyme. The vector containing the horse Cyt*c* cDNA sequence was a kind gift of Dr. Lucy Waskell (University of Michigan) (*15*). The horse Cyt*c* sequence was removed by restriction digestion with *Nco*I and *Bam*HI. Rodent Cyt*c* cDNA was amplified from total rat muscle cDNA using *Nco*I and *Bam*HI restriction site-containing primers 5′-AATTTACCATGGGTGATGTTGAAAAAG-3′ (forward primer) and 5′-AATAAAGGATCCAGTGGAATTATTCAT-3′ (reverse primer). Following restriction digestion with *Nco*I and *Bam*HI, the fragment was cloned into the similarly treated pLW01 vector, and the sequence was confirmed by sequencing. Site-directed mutagenesis was employed to generate the two mutant constructs. In order to introduce the mutations, the oligonucleotides 5′-AGGCTGCTGGATTCTCT**TTC**ACAGATGCCAACAAGAACAAAGG-3′ (Tyr48Phe) and 5′-AGGCTGCTGGATTCTCT**GAC**ACAGATGCCAACAAGAACAAAGG-3′ (Tyr48Glu) were used in combination with the QuikChange site-directed mutagenesis kit (Stratagene, Agilent Technologies, La Jolla, CA) according to the manufacturer's protocol. Successful introduction of mutations was confirmed by sequencing. A specific *Escherichia coli* strain, C41 (DE3) (*16*), was then used to overexpress the Cyt*c* variants. The plasmids were transformed into the competent OverExpress C41 (DE3) *E. coli* cells (Lucigen, Middleton, WI) according to supplier's protocol. Selected clones were inoculated into 10 mL of TB medium (Difco, BD, Franklin Lakes, NJ) containing 0.24 mM carbenicillin and grown overnight at 37 °C under constant shaking. The suspension was then distributed into several flasks containing a total of 5 L of carbenicillin-containing TB medium and grown until an OD_{600} of 2−3 was reached. At this time, Cyt*c* expression was induced by addition of 100 mM IPTG. Protein overexpression was continued for 8 h, and cells were then harvested by 20 min centrifugation at 27000*g* at 4 °C. Bacterial pellets were immediately frozen and stored at −80 °C.

Extraction and Purification of Cytochrome c. The bacterial pellets were resuspended in B-Per reagent (Pierce, Rockford, IL), supplemented with 1 mM PMSF and lysozyme (30 mg/L), and extracted according to the manufacturer's protocol. Extracted proteins were separated from the cell debris by 40 min centrifugation at 27000*g* at 4 °C. Cyt*c* was subsequently purified by a two-step ion-exchange chromatography procedure modified from ref *10*. The extract was adjusted to pH 7.5, diluted with ddH_2O until a conductance of 4 mS/cm was reached, and applied to a DE anion-exchange column (Whatman, Piscataway, NJ) equilibrated to a similar conductance with 20 mM phosphate buffer, pH 7.5. The majority of bacterial proteins bound to the column, whereas overexpressed Cyt*c* was collected in the flow-through. The solution was adjusted to pH 6.5 with HCl, and conductance was increased to 6 mS/cm by addition of KH_2PO_4 and loaded onto a CM cellulose cation-exchange column (Whatman) equilibrated with 40 mM phosphate buffer, pH 6.5. After the cation-exchange column was washed, Cyt*c* was eluted with 0.5 M NaCl in 40 mM phosphate buffer, pH 6.5. Fractions without any apparent impurities, as judged by SDS−PAGE/Coomassie R-250 staining, were pooled and desalted/concentrated by centrifugation using Amicon Ultra-15 3k units (Millipore, Billerica, MA). Enzyme preparations were aliquoted and stored at −80 °C. There were no indications of artificial Cyt*c* phosphorylation due to overexpression using the bacterial system as confirmed by Western analysis with anti-phosphoSer/Thr/Tyr antibodies as described (*11*) (not shown).

Analysis of Cytochrome c Absorption Spectra. Cyt*c* was oxidized with $K_3Fe(CN)_6$ and desalted using NAP-10 columns (GE Healthcare, Piscataway, NJ). Absorption spectra were recorded on a Jasco V-570 double beam spectrophotometer (2 nm bandwidth, 200 nm/min scanning speed). Reduced Cyt*c* was obtained by addition of sodium dithionite, removal of reductant via NAP-10 columns, and spectra acquisition as described above.

Measurements of Cytochrome c Redox Potential. The midpoint redox potential ($E^{0\prime}$) was analyzed spectrophotometrically by the equilibration method according to ref *17* using as a reference compound 2,6-dichloroindophenol (DCIP, $E^{0\prime}$ = 237 mV), which has an absorption band at 600 nm in its oxidized state. One milliliter of Cyt*c* solution (2 mg/mL) was mixed in a large spectrophotometric cuvette with 2 mL of 50 mM citrate buffer, pH 6.5, 0.1 mL of 1 mM DCIP, and 25 μL of 1 mM $K_3Fe(CN)_6$ to fully oxidize Cyt*c*. Absorbances corresponding to fully oxidized Cyt*c* ($A_{550}-A_{570}$) and DCIP (A_{600}) were recorded using a Jasco V-570 double beam spectrophotometer. The mixture was then sequentially reduced by 3 μL additions of 10 mM ascorbate (pH 6.5), and absorbance values were acquired at each step. When readings became constant, a few grains of $Na_2S_2O_4$ were added to fully reduce Cyt*c* and DCIP. For each step, ratios of oxidized and reduced forms of both compounds were calculated. Data obtained were plotted as $\log(DCIP_{OX}/DCIP_{RED})$ versus $\log(Cyt_{OX}/Cyt_{RED})$, yielding a linear graph with a slope of n_{DCIP}/n_{Cyt} and a *y*-axis intercept of $n_{Cyt}/59.2(E_{Cyt} - E_{DCIP})$. These values were used to calculate the $E^{0\prime}$ of Cyt*c* from the Nernst equation.

Kinetic Measurements of Cytochrome c Oxidation by Cytochrome c Oxidase. Regulatory-competent CcO was isolated from bovine liver and heart under conditions preserving its phosphorylation status as previously described (*18*). A CcO

aliquot was diluted to 3 μM final concentration in the presence of a 40-fold molar excess of cardiolipin and 0.1 mM ATP in CcO measuring buffer (10 mM K-HEPES (pH 7.4), 40 mM KCl, 2 mM EGTA, 10 mM KF, 1% Tween 20) and dialyzed overnight at 4 °C to remove cholate bound to CcO during enzyme purification. CcO respiration (150 nM) was analyzed in a closed chamber equipped with a micro Clark-type oxygen electrode (Oxygraph system; Hansatech, Pentney, U.K.) at 25 °C in 400 μL of CcO measuring buffer and 20 mM ascorbate as electron donor. Increasing amounts of purified Cyt*c* mutants (0−15 μM) were added, and oxygen consumption was recorded and analyzed with the Oxygraph software (Hansatech). The activity was expressed as turnover number (TN) (s^{-1}).

Caspase-3 Activity Induction by Purified Cytochrome c. The ability of purified Cyt*c* to induce caspase-3 activation was assayed using an *in vitro* approach with cell-free extracts essentially as described (*19*). Extracts representing cytoplasmic cell fractions were prepared from cultured HeLa, Cyt*c* −/− (ATCC, CRL 2613), and a breast cancer cell line BT5419 (kind gift of Dr. H. R. Kim, Wayne State University). After trypsinization, cells (8×75 cm^2 flasks) were pelleted and washed twice with PBS, followed by one wash with cell extract buffer (CEB: 20 mM HEPES, pH 7.5, 10 mM KCl, 1.5 mM $MgCl_2$, 1 mM EDTA, 1 mM EGTA, 1 mM dithiothreitol, 100 μM PMSF). Two volumes of CEB were added to the cell pellet, and the suspension was transferred to a 2 mL Dounce homogenizer and allowed to swell in the hypotonic CEB for 15 min. Subsequently, cells were disrupted by 20 strokes with a tight pestle. Lysates were centrifuged at 15000*g* for 15 min at 4 °C to remove nuclei and organelles. Afterward, protein concentration of the extracts was measured using the D_c protein assay (Bio-Rad, Hercules, CA). Extracts were aliquoted and stored frozen at −80 °C until further use. Caspase-3 activity, induced by addition of purified Cyt*c*, was measured using the EnzChek Caspase-3 assay kit (Invitrogen, Carlsbad, CA) employing the rhodamine 110-linked DEVD tetrapeptide (artificial substrate of caspase-3), which fluoresces upon cleavage by caspase-3. Initial tests revealed that caspase-3 activity in the extracts is maximally stimulated with Cyt*c* concentrations above 15 μg/mL. Cell extracts were diluted to a protein concentration of 2 mg/mL (HeLa, BT5419) or 1 mg/mL (Cyt*c* −/−) and incubated with oxidized wild-type, Tyr48Phe, and Tyr48Glu Cyt*c* variants (0, 20, and 40 μg/mL) for 2 h at 37 °C. Ten microliter aliquots of preincubated (activated) extracts were then assayed for caspase-3 activity in triplicate, and in parallel in triplicates containing a caspase-3 inhibitor according to the manufacturer's protocol. Fluorescence was detected using a Fluoroskan Ascent FL plate reader (Labsystems, Thermo Scientific, Waltham, MA), excitation filter 485 nm/14 nm bandwidth, emission filter 527 nm/bandwidth 10 nm. Fluorescence values were acquired in 30 min intervals for 3 h. Amount of cleaved substrate was calculated from the rhodamine 110 calibration curve, and data were expressed in pmol of DEVD·min^{-1}·(mg of protein)$^{-1}$. Signal from wells containing caspase inhibitor was subtracted from the results, as was background activity in extracts that were not treated with Cyt*c*.

Generation of Small Unilamellar Liposomes. 1,2-Dioleoyl-*sn*-glycero-3-phosphocholine (PC), 1,1′,2,2′-tetraoleoylcardiolipin (CL), and 1-oleoyl-2-[12-[(7-nitro-2,1,3-benzoxadiazol-4-yl)amino]dodecanoyl]-*sn*-glycero-3-phosphocholine (NBD-PC) were obtained from Avanti Polar Lipids, Inc. (Alabaster, AL). 1,1′,2-Trioleoyl-2′-[12-[(7-nitro-2,1,3-benzoxadiazol-4-yl)amino]-dodecanoyl]cardiolipin (NBD-CL) was custom-synthesized by Avanti Polar Lipids, Inc. (Alabaster, AL). Individual phospholipids, stored in chloroform, were mixed and dried under nitrogen. Then lipids were solubilized by vortexing in HEPES buffer (20 mM, pH 7.4) and sonicated three times for 30 s on ice. Liposomes were used immediately after preparation. Distribution of NBD-CL and NBD-PC between the inner and outer leaflets of the liposomes was estimated using the reducing agent sodium dithionite as described (*20*).

Binding of Cytochrome c to Liposomes. Binding was monitored by quenching of fluorescence of NBD-CL. NBD-CL (1 mol %) was incorporated into PC and PC/CL liposomes. A Shimadzu spectrofluorometer RF-5301PC was employed for fluorescence measurements using a 0.2 mL quartz cuvette. NBD-CL fluorescence was detected using excitation and emission wavelengths of 470 and 537 nm, respectively. Fluorescence quenching was detected upon addition of Cyt*c* aliquots (12.5 nM) to liposomes containing 20 μM phospholipids in HEPES buffer (20 mM, pH 7.0). The Cyt*c*/liposome mixture was incubated for 3 min to achieve equilibration of protein/lipid binding.

Peroxidase Activity of Cytochrome c. For the following experiments, the concentration of Cyt*c* stock solutions was determined with the modified Lowry protein assay kit (Pierce, Rockford, IL) in the presence of 0.06% SDS. Cyt*c* peroxidase activity was determined by measuring the oxidation rate of Amplex Red (*N*-acetyl-3,7-dihydroxyphenoxazine; Invitrogen, Carlsbad, CA) to the fluorescent product resorufin. Cyt*c* (0.5 μM) was preincubated with liposomes (25 μM phospholipids) in HEPES buffer (20 mM, pH 7.0) for 10 min. The peroxidase reaction was started by addition of Amplex Red (10 μM) and H_2O_2 (50 μM) or 13*S*-hydroperoxy-9*Z*,11*E*-octadecadienoic acid ((13S)HpODE; Cayman Chemical, Ann Arbor, MI; 10 μM). The rate of peroxidase reaction was calculated based on data collected within 20 s using a Shimadzu spectrofluorometer RF-5301PC with excitation and emission wavelengths of 575 and 585 nm, respectively.

Assessment of Oxidized Molecular Species of CL by Mass Spectrometry. To assess different oxidized molecular species of CL, electrospray ionization−liquid chromatography−mass spectrometry (ESI-LC-MS) was performed using a Dionex Ultimate 3000 HPLC coupled online to an ESI ion source and a linear ion trap mass spectrometer (LXQ Thermo-Fisher) with the Xcalibur operating system (Thermo Fisher Scientific, San Jose, CA). CL and its oxidized molecular species were extracted by the Folch procedure (*21*) and separated on a normal phase column (Luna 3 μm silica 100A, 150 × 2 mm; Phenomenex, Torrance, CA) with a flow rate of 0.2 mL/min applying a gradient elution using solvents containing 5 mM CH_3COONa (A, *n*-hexane:2-propanol:water, 43:57:1 (v/v/v); and B, *n*-hexane:2-propanol:water, 43:57:10 (v/v/v)). Analysis of (hydroperoxy and hydroxy) oxidized phospholipid species was performed as described (*22*).

RESULTS

Purification of Functional and Correctly Folded Cytochrome c Mutants Overexpressed in C41 (DE3) E. coli Cells. Replacement of an amino acid that can be phosphorylated with the negatively charged (and thus phosphomimetic) residues Asp or Glu is a commonly used method to study the effects of protein phosphorylations *in vitro*. Such phosphomimetic substitutions often result in functional changes similar to those caused by *in vivo* protein phosphorylation. This approach, which was chosen for this study, was successfully applied to numerous

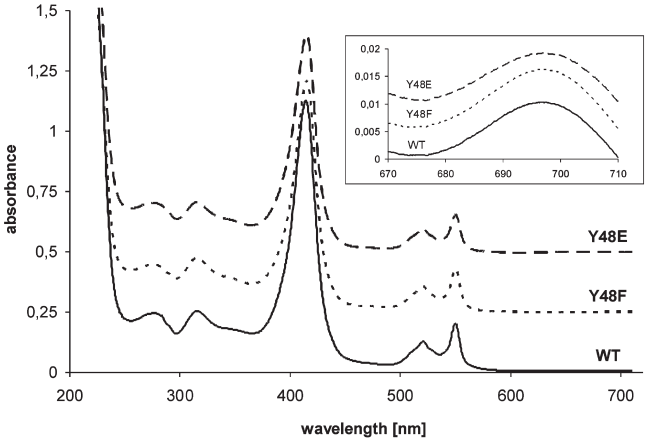

FIGURE 1: Absorption spectra of purified cytochrome *c* variants. Ten micromolar wild-type (WT), Tyr48Phe (Y48F), and Tyr48Glu (Y48E) cytochromes were reduced with sodium dithionite and desalted, and spectra were acquired using a Jasco V-570 double beam spectrophotometer. For presentation, the individual spectra were shifted from each other by 0.25 unit along the *y*-axis. The presence of the 695 nm peak in the cytochromes' oxidized state is shown in the insert, where the individual spectra are shifted by 0.005 unit from each other.

mitochondrial proteins (*23*, *24*), including a recent study on OxPhos component ATP synthase (*25*).

We overexpressed and purified wild-type, Tyr48Phe, and Tyr48Glu Cyt*c*. Our two-step ion-exchange chromatography procedure yielded 15−20 mg of purified Cyt*c* per liter of bacterial culture. The preparations were without any apparent impurities as judged by SDS−PAGE/silver staining (Supporting Information Figure 1) and analysis by spectrophotometer (Figure 1), with 410 nm/280 nm ratios of >4 for all three overexpressed and purified Cyt*c* fractions as an indicator and marker value for Cyt*c* purity (*26*). The wild type and both of the Tyr48Phe and Tyr48Glu mutant proteins were fully reducible according to absorption spectra measurements (Figure 1). Moreover, all protein preparations were purified in the correctly folded conformation ("state III") (*27*), as evidenced by the presence of the weak 695 nm absorption peak in the oxidized state of Cyt*c*, caused by the bond between Met80 and the heme iron (Figure 1, insert). This peak is readily lost upon any harmful treatment to the enzyme and was named an "indicator of trouble" (*27*).

The Midpoint Redox Potential Is Reduced in the Cytochrome c Tyr48Glu Mutant. As an initial characterization, we measured the enzyme midpoint redox potential ($E^{0'}$) in order to evaluate the thermodynamic feasibility of Cyt*c* mutants' proper function within the respiratory chain. We tested our hypothesis that Cyt*c* phosphomimetic mutation Tyr48Glu, located in close proximity to the heme redox center, leads to alteration of the redox potential. Cyt*c* redox potential values reported in the literature range between 220 and 270 mV for mammalian Cyt*c* (*17*, *28*) and are approximately midway between the redox potentials of complexes III and IV. Thus Cyt*c* may efficiently function as a mobile carrier of electrons between these complexes. Control $E^{0'}$ measurements of bovine heart Cyt*c* via the equilibration method using DCIP yielded values within the published range (data not shown). The wild-type redox potential value of our overexpressed rodent Cyt*c* of 237 ± 11 mV was similar to literature values; both mutants, however, displayed significantly decreased redox potentials (Figure 2). The $E^{0'}$ of the Tyr48Phe was 207 ± 7 mV, and an even more pronounced decrease was observed in the case of the Tyr48Glu mutant (192 ± 5 mV). These data indicate a

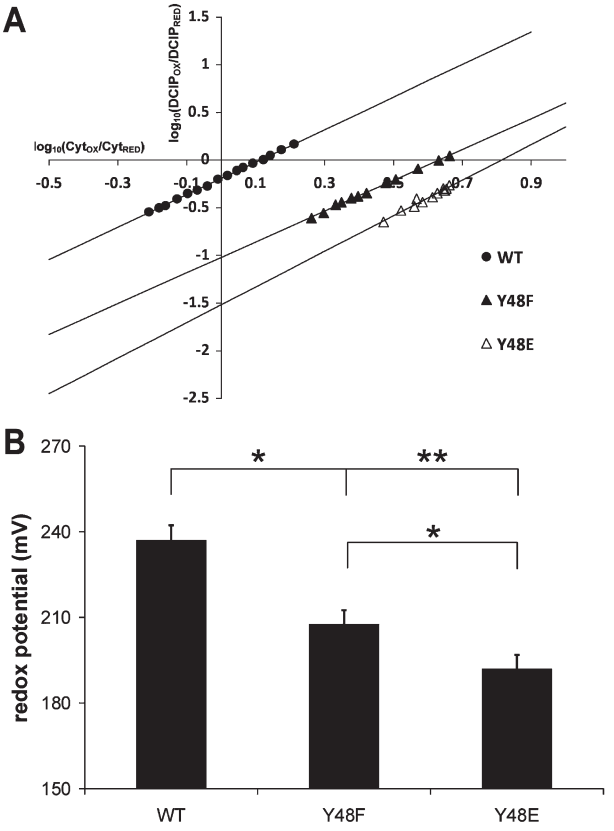

FIGURE 2: Redox potential of cytochrome *c* variants. Redox potential of Cyt*c* variants (40 μM) was assessed spectrophotometrically using DCIP (20 μM) as equilibration redox substrate. (A) Data obtained were plotted as $\log(DCIP_{OX}/DCIP_{RED})$ versus $\log(Cyt_{OX}/Cyt_{RED})$, yielding a linear graph with a slope of n_{DCIP}/n_{Cyt} and a *y*-axis intercept of $n_{Cyt}/59.2(E_{Cyt} - E_{DCIP})$. One representative titration is shown for each Cyt*c* variant. (B) Titration values were used to calculate $E^{0'}$ of Cyt*c* variants using the Nernst equation from the intercept and slope of the linear line fitted through the experimental data. Calculated values are expressed as means ± SD ($n = 3$; *, $p < 0.05$; **, $p < 0.01$).

decrease of the Cyt*c* redox potential by the Tyr48Glu mutation to values matching those of complex III, which may lead to an inhibition of electron flux in the ETC.

Decreased Rate of Tyr48Glu Mutant Cytochrome c Oxidation in the Reaction with Isolated Cytochrome c Oxidase. The Tyr48 phosphorylation of Cyt*c* was discovered in bovine liver tissue *in vivo*, and such phosphorylation resulted in about 50% inhibition in the reaction with CcO at maximal turnover (*11*). Therefore, as a functional test of the purified Cyt*c* mutants, we measured the kinetics of Cyt*c* oxidation by bovine liver CcO, which was isolated under conditions that preserve the *in vivo* phosphorylation status and thus yield a regulatory-competent enzyme (*18*). Measuring oxygen consumption using such an enzyme should therefore provide a physiologically realistic *in vitro* environment to assess the possible effect of the phosphomimetic Tyr48Glu mutation.

The measurements of CcO activity with purified Cyt*c* mutants as substrates revealed that CcO oxidizes the Tyr48Glu enzyme at lower rates compared to the wild type or the Tyr48Phe mutant. Interestingly, we observed qualitatively similar results as were previously obtained with Tyr48-phosphorylated Cyt*c* purified from bovine liver in that the curve is hyperbolic and the maximal velocity is decreased by 30% compared to wild type (Figure 3A), suggesting that the phosphomimetic mutant is an adequate

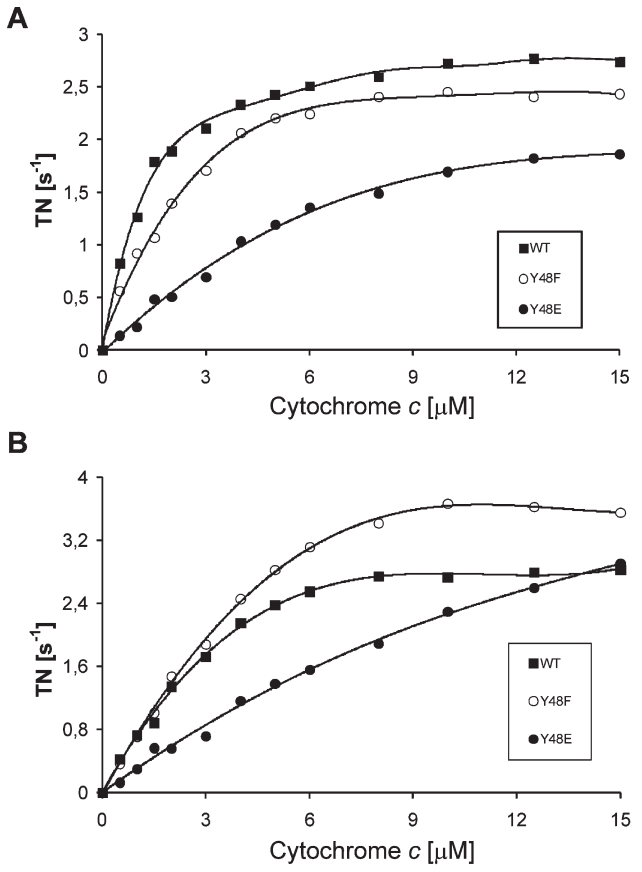

FIGURE 3: CcO activity with purified cytochrome *c*. Oxygen consumption of (A) bovine liver CcO (0.15 μM) or (B) bovine heart CcO (0.15 μM) was measured using the Oxygraph system (Hansatech) at increasing concentrations (1−15 μM) of purified wild-type, Tyr48-Glu (Y48E), and Tyr48Phe (Y48F) Cyt*c*. K_M values (μM) of CcO for Cyt*c* are as follows: 1.1 (wild type), 3.7 (Y48E), and 1.7 (Y48F) with liver CcO (A) and 2.0 (wild type), 5.8 (Y48E), and 2.7 (Y48F) with heart CcO (B). Data are expressed as turnover number (s^{-1}). Shown are representative measurements ($n = 3$ each).

system for studying Cyt*c* functionality. In addition, the apparent K_M is increased from 1.1 (wild type) to 3.7 (Tyr48Glu).

We further analyzed the kinetics of the purified Cyt*c* variants using isolated CcO from cow heart tissue, which contains heart-specific isoforms of CcO subunits VIa, VIIa, and VIII. Interestingly, unlike the situation with liver CcO, the Tyr48Glu mutant showed a lower affinity to heart CcO compared to the wild-type or the Tyr48Phe mutant Cyt*c*, and the apparent K_M of Tyr48Glu Cyt*c* is almost 3-fold increased (5.8 vs 2.0 μM of the wild type). However, the maximal turnover of all three Cyt*c* variants is similar (Figure 3B).

Tyr48Glu Mutant Cytochrome c Is Incapable of Activating Caspase-3. As a functional test to directly assess the effect of Tyr48 substitution on apoptosis, we analyzed the ability of Cyt*c* to initiate apoptosis by downstream activation of caspase-3 as a consequence of apoptosome assembly. We incubated increasing concentrations of the purified Cyt*c* variants with the cytosolic fractions of HeLa, mouse Cyt*c* −/−, and breast cancer cell line BT5419 and measured activation of caspase-3 by subsequent cleavage of the artificial tetrapeptide substrate DEVD coupled to fluorescent rhodamine. The wild-type and Tyr48Phe cytochromes induced caspase-3 activity to a similar extent (Figure 4). Strikingly, the Tyr48Glu was unable to induce any measurable DEVD cleavage using cytosolic fractions of HeLa cells and cytochrome *c* −/− cells (Figure 4) or BT5419 breast cancer cells

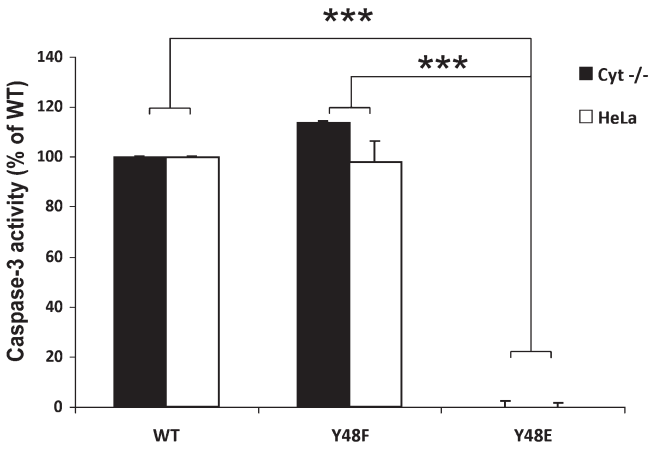

FIGURE 4: Cytochrome *c*-induced caspase-3 activity. Cytosolic fractions of Cyt −/− (1 mg/mL of protein) or HeLa cells (2 mg/mL of protein) were incubated with variants of Cyt*c* (20 μg/mL) for 2 h. Cleavage of the artificial substrate DEVD-R110 via induced caspase-3 activity was measured in 10 μL aliquots in triplicate. Data were recalculated relative to wild-type Cyt*c*, expressed as means ± SD. The ability to induce caspase-3 activation is abolished in the Tyr48Glu mutant (***, $p < 0.001$).

(data not shown). These data suggest that the *in vivo* Tyr48 phosphorylation might have a similar effect and serve as a potent antiapoptotic regulatory mechanism.

Tyr48Glu Mutant Cytochrome c Binds to Cardiolipin with Decreased Affinity and Displays Lower Peroxidase Activity in the Presence of Cardiolipin. In mitochondria, Cyt*c* binds to anionic phospholipids, particularly cardiolipin. This interaction causes a partial unfolding of the enzyme upon which Cyt*c* acquires peroxidase activity. The peroxidase activity of Cyt*c* has been implicated in regulating its release from the mitochondria during apoptosis. As this activity involves a tyrosine radical (*29*), we tested the possibility that the phosphomimetic Tyr48Glu substitution may affect peroxidase activity, if the tyrosine radical most proximal to the heme center participates in cardiolipin peroxidation.

Binding of Cyt*c* to the membranes can be estimated using several techniques including analysis of spectral properties of Cyt*c*, physical properties of the membranes, and lipid/protein mobility (*29*−*31*). Here, we studied the direct Cyt*c*−cardiolipin interactions using cardiolipin that was labeled with the fluorescent NBD moiety (NBD-CL), by following analysis of quenching of NBD fluorescence upon protein binding. As a control lipid we included 1,2-dioleoyl-*sn*-glycero-3-phosphocholine (PC) labeled with NBD (NBD-PC). The NBD group of the phospholipid conjugate is located near the membrane interface, and Cyt*c* binding to the membrane can quench NBD fluorescence via efficient resonance energy transfer from NBD to heme and due to disturbance of the NBD environment by interaction with amino acids of Cyt*c* (*20*, *32*). As shown in Figure 5A there was a very minor decay in NBD-PC fluorescence upon addition of wild-type or mutant Cyt*c* to NBD-PC-containing liposomes. Substitution of NBD-CL for NBD-PC produced a notable fluorescence decay, which was concentration dependent. Maximum effect was observed at 20 mol % CL (Figure 5B). The quenching curves were nonlinear and saturated at the Cyt*c*:phospholipid ratio of 1:50; at this protein:lipid ratio fluorescence was quenched by about 70% for wild-type and Tyr48Phe Cyt*c* (Figure 5B). Concentration dependence of fluorescence quenching was altered in the Tyr48Glu mutant. The latter was able to induce only a 55% fluorescence

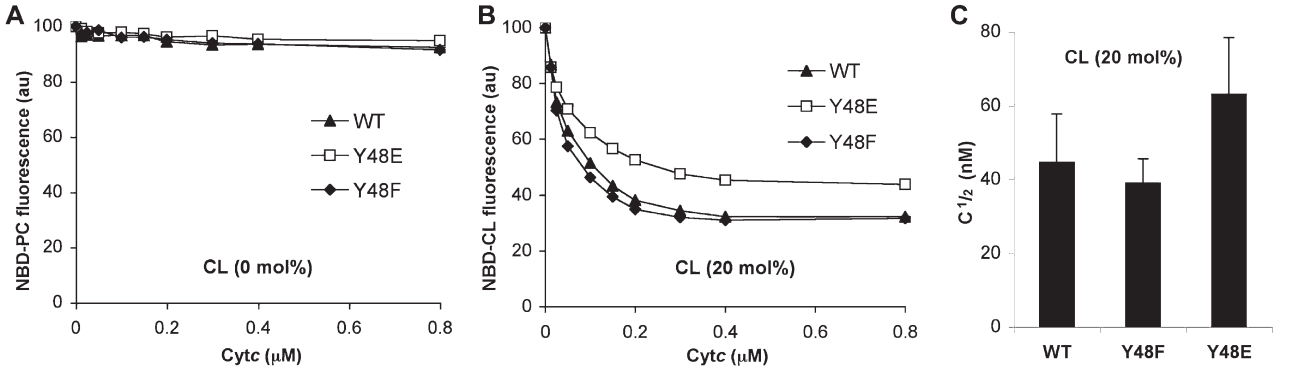

FIGURE 5: Cardiolipin binding to cytochrome *c*. 1,2-Dioleoyl-*sn*-glycero-3-phosphocholine (PC) or cardiolipin (CL), which were labeled with the fluorescent group NBD (NBD-PC and NBD-CL, respectively) and incorporated into liposomes to analyze quenching of NBD-PC and NBD-CL fluorescence by Cyt*c* binding. (A) Liposomes containing 20 μM PC and 0.2 μM NBD-PC and (B) liposomes containing 16 μM PC, 4 μM CL, and 0.2 μM NBD-CL were used. Wild type (WT, closed triangles), Tyr48Glu (Y48E, open squares), and Tyr48Phe (Y48F, closed diamonds). (C) Based on the quenching titration curves the concentration of Cyt*c* was determined that resulted in a 50% reduction (quenching) of fluorescence ([$C_{1/2}$]). The reverse value ([$C_{1/2}$]$^{-1}$) is proportional to the affinity constant of binding. The WT and Y48F variants showed similar binding to Cyt*c*, whereas binding affinity is about 31% reduced in the Y48E mutant.

decay at high Cyt*c* concentrations, and 1.5-fold higher concentrations of Tyr48Glu mutant Cyt*c* as compared to wild-type Cyt*c* were required to cause half-maximal fluorescence quenching (Figure 5C). Based on the data we estimated that Tyr48Glu Cyt*c* has 31% lower affinity to bind CL, whereas wild-type and Tyr48Phe Cyt*c* show similar affinities.

Cyt*c* can oxidize different substrates using hydroperoxides as oxidizing equivalents. Native Cyt*c* displays a weak peroxidase activity that is markedly enhanced upon binding of CL (*33*). The peroxidase activity of Cyt*c* was then assayed directly by measuring the oxidation rate of Amplex Red by 0.5 μM Cyt*c*, with H_2O_2 (Figure 6A) or the lipid peroxide substrate 13(S)HpODE (Figure 6B). Background peroxidase activity of wild-type and mutant Cyt*c* was nearly zero in the absence of peroxides (data not shown). In the absence of cardiolipin, activity with H_2O_2 as a substrate was 2-fold higher in the Tyr48Glu mutant compared to either wild-type or Tyr48Phe Cyt*c* (Figure 6A). Peroxidase activity was about 2-fold induced in wild-type and Tyr48Phe mutant Cyt*c* in the presence of tetraoleoyl-CL (20%). In contrast, no such induction was observed in the Tyr48Glu mutant (Figure 6A). Of note, oleoyl-containing fatty acid residues cannot be readily oxidized by Cyt*c*. Therefore, binding of tetraoleoyl-CL facilitates peroxidase activation but does not compete with the oxidizable substrates. With 13(S)HpODE as a source of oxidizing equivalents, a significant enhancement of peroxidase activity was observed in wild-type (> 100-fold) and Tyr48Phe Cyt*c* (3.7-fold) in the presence of cardiolipin (20%), but no such CL-dependent induction was found in the phosphomimetic mutant (Figure 6B). Notably, the phosphomimetic mutant showed higher baseline levels of peroxidase activity in the absence of CL, and the induction of peroxidase activity was only observed in the presence of liposomes containing higher levels of CL (50%). As discussed below, it is possible that the presence of a negatively charged group in proximity to Asn52 partially mimics the effect of CL on this domain of Cyt*c*, thus altering dependence of its peroxidase activity on the addition of CL in the Tyr48Glu mutant. Moreover, the substitution of Tyr48 for a negatively charged Glu residue may be associated with the decreased CL binding to Cyt*c*. This is further supported by a recent study (*34*) suggesting that the local environment of Tyr48 may be involved in CL binding.

Next, we assessed peroxidase and oxygenase activities of Cyt*c*/CL complexes using an oxidizable substrate, tetralinoleylcardiolipin

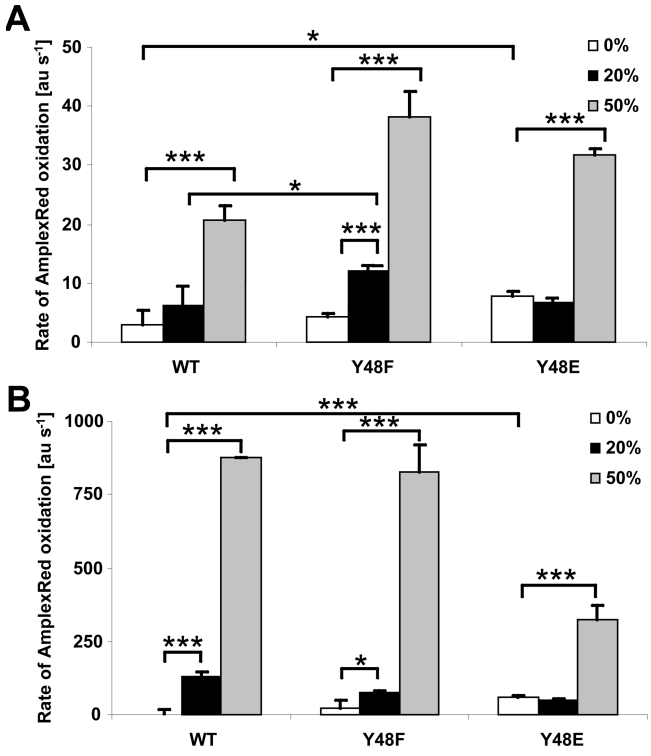

FIGURE 6: Cytochrome *c* peroxidase activity. Cyt*c* peroxidase activity was determined via the rate of AmplexRed oxidation to the fluorescent product resorufin. Cyt*c* (0.5 μM) was incubated with AmplexRed (10 μM) and liposomes (with total of 25 μM phospholipids) containing 0%, 20%, or 50% cardiolipin (CL), in the presence of (A) H_2O_2 (50 μM) or (B) the lipid peroxide substrate 13(s)HpODE (10 μM). Data are expressed as means ± SD. In the presence of CL, Cyt*c* peroxidase activity is significantly induced in the wild type and Y48F mutant (*, $p < 0.1$; ***, $p < 0.01$); in contrast, induction of peroxidase activity in the phosphomimetic mutant was observed only in the presence of liposomes containing 50% CL.

(TLCL). To characterize these two distinct enzymatic activities, we employed ESI-LC-MS to measure hydroperoxy-TLCL and hydroxy-TLCL products formed in the course of these two Cyt*c*-driven reactions in the presence of H_2O_2 (*22*, *35*). Representative ESI-LC-MS spectra of TLCL, oxidized by both wild-type and Tyr48Glu mutant Cyt*c*, are presented in Figure 7. LC-MS analysis revealed molecular species of mono-, di-, tri-, and tetrahydroperoxy molecular species of CL (products of the *oxygenase reaction*) that were

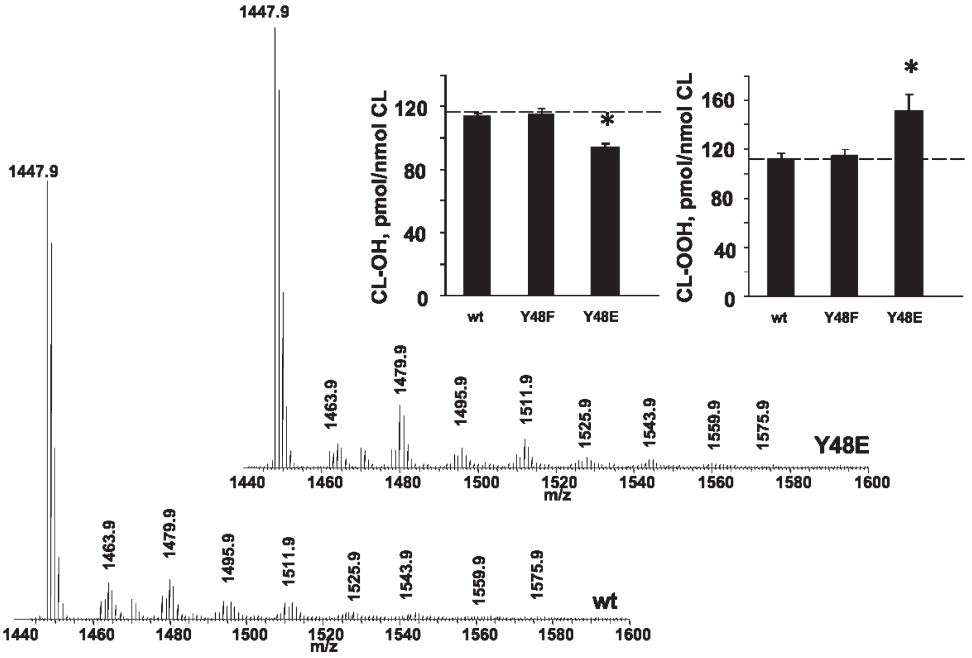

FIGURE 7: Oxidation of tetralinoleylcardiolipin by cytochrome *c*. Cyt*c* (5 μM) was incubated with liposomes (with a total of 250 μM phospholipids) containing 20% tetralinoleylcardiolipin (TLCL), in the presence of H_2O_2 (100 μM) in 20 mM HEPES, pH 7.4, and 100 μM DTPA for 10 min at 37 °C. After incubation lipids were extracted and resolved by ESI-LC-MS. Representative ESI-LC-MS spectra of TLCL incubated in the presence of either wild-type (wt) or Tyr48Glu mutant (Y48E) Cyt*c*. Insert: Accumulation of hydroxy (left panel) and hydroperoxy (right panel) molecular species of tetralinoleylcardiolipin formed in the presence of either wild-type Cyt*c* or Cyt*c* mutants. Data are expressed as means ± SD, $n = 3$. *$p < 0.05$, versus wild-type Cyt*c*.

represented by molecular ions with *m*/*z* 1479.9, 1511.9, 1543.9, and 1575.9, respectively. In addition, molecular ions of mono-, di-, tri-, and tetrahydroxy molecular species of TLCL (products of the *peroxidase reaction*) with *m*/*z* 1463.9, 1495.9, 1525.9, and 1559.9 were detected in the mass spectra (Figure 7). Quantitative assessment of TLCL oxidation products showed that accumulation of hydroperoxy and hydroxymolecular species of TLCL was similar after incubation with either wild-type or Tyr48Phe mutant Cyt*c* (Figure 7, insert). Hovewer, the level of hydroxy species of TLCL formed in the presence of Tyr48Glu mutant Cyt*c* was significantly lower as compared to wild-type and Tyr48Phe mutant Cyt*c* (Figure 7, insert, left panel). This indicates that the peroxidase activity of the mutant was suppressed. Interestingly, significantly higher amounts of hydroperoxy-TLCL were detected when TLCL was incubated with Tyr48Glu mutant Cyt*c* as comared to wild-type or Tyr48Phe mutant Cyt*c* (Figure 7, insert, rigth panel). These results indicate that conversion of Tyr48 into Glu differently affects peroxidase and oxygenase activities of Cyt*c*/CL complexes. Oxygenase activity is directed toward nonoxidized CL that binds, most likely, in the region of the Cyt*c* molecule in the vicinity of Lys71, Lys73 and Tyr67, Tyr74 (*36*−*38*). In contrast, the peroxidase reaction utilizes peroxidized CL (hydroperoxy-CL) as a source of oxidizing equivalents. While the exact binding site for hydroperoxy-TLCL on Cyt*c*/TLCL complex is not known, it is likely that it is close to the binding site of fatty acid hydroperoxides, in the neighborhood of Tyr48 (*39*). This explains, at least in part, the similarity of the effects of the phosphomimetic Tyr48Glu substitution on peroxidase activities analyzed utilizing 13(S)HpODE (Figure 6B) and hydroperoxy-TLCL as substrates.

DISCUSSION

In the last 2 decades, our view of Cyt*c* has radically changed from a faithful electron carrier in the respiratory chain to a multifunctional enzyme involved in cellular life and death decisions. The discovery of two phosphotyrosines in Cyt*c* has contributed to this paradigm shift by demonstrating that Cyt*c*, as a target of signaling pathways, is integrated into regulatory networks of eukaryotic cells. The present biochemical characterization of the Tyr48Glu mutant, mimicking the liver-type phosphorylation, versus the wild-type and Tyr48Phe enzyme variants, provides insights into the effect of tyrosine phosphorylation.

A reason for the decreased redox potential of the phosphomimetic Tyr48Glu mutant may be a perturbation of the heme environment. It has long been noted that any Cyt*c* derivatives that open the heme crevice, exposing it to the polar aqueous environment, stabilize the iron in its oxidized state (*27*). Introduction of a negative charge at the Tyr48 position via mutation, or by phosphorylation *in vivo*, is likely to cause such a disturbance, leading to the observed decrease of the redox potential by 45 mV in the Tyr48Glu mutant. In addition, Tyr48 is involved in heme stabilization by hydrogen bonding of the heme propionate group (*27*), and the loss of the hydroxyl group in the Tyr48Phe mutant may account for the less pronounced decrease of the redox potential in this Cyt*c* variant. Indeed, a similarly decreased redox potential was previously observed in other Tyr mutants of human Cyt*c* in a study analyzing the role of tyrosine nitration (*40*). Shifting the redox potential of Cyt*c* below 200 mV, which is less than the redox potential of cytochrome c_1 of respiratory complex III, suggests that modifying Cyt*c* by phosphorylation of Tyr48 may inhibit its main function as an electron carrier between complexes III and IV. Perhaps "relieving" Cyt*c* from electron transport in the respiratory chain may favor its involvement in electron transport to or from its other mitochondrial redox partners, such as reduction by superoxide (*7*). This redox reaction occurs only when Cyt*c* is not tethered to the outer leaflet of the inner mitochondrial membrane (*41*), which may be the case for the Tyr48-phosphorylated species, since our experiments showed decreased binding affinity of the Tyr48Glu mutant

toward its typical lipid ligand cardiolipin. Cyt*c* reduced by superoxide could then feed the electron into CcO or reduce $p66^{Shc}$, a recently discovered redox partner, leading to production of H_2O_2 (*8*).

Our previous studies on *in vivo* Tyr48-phosphorylated Cyt*c* isolated from bovine liver revealed that this modification decreases the maximal turnover of Cyt*c* oxidation with isolated liver CcO by 50% (*11*). The present data on Tyr48Glu-mutated Cyt*c* closely mimic our previous findings. The decrease in respiration rate (by 30%) was not as pronounced as with *in vivo* phosphorylated Cyt*c*. However, the phosphotyrosine moiety is more bulky compared to the glutamate substitution, which may account for the difference in magnitude of the response. Surprisingly, a decreased V_{max} of Tyr48Glu mutant oxidation was not observed with a preparation of heart CcO, suggesting a tissue-specific "sensing" of the Cyt*c* modification, perhaps caused by the presence of the heart-specific isoforms of 3 out of the 13 subunits of CcO. However, an increased K_M was observed, mimicking the effect of *in vivo* Tyr97 phosphorylated Cyt*c* isolated from bovine heart (*10*).

In mitochondria, a portion (10−15%) of Cyt*c* is bound to the limited CL pool on the outer leaflet of the inner mitochondrial membrane (*33*). However, during preapoptotic events, a considerable portion of CL from the outer mitochondrial membrane becomes available for Cyt*c* binding, causing partial unfolding of the enzyme, triggering its peroxidase activity (*33*, *42*). The interaction between Cyt*c* and CL is complex. It is initiated by electrostatic interaction between the positively charged lysine residues of Cyt*c* and the negatively charged phosphate moiety of CL and by hydrophobic interactions of one of the fatty acid chains of CL with the hydrophobic pocket on Cyt*c*. A putative hydrogen bond between Asn52 and CL further tightens the interaction (*42*). Our observation of decreased binding affinity of the Tyr48Glu mutant to cardiolipin might be attributed to perturbation of the above-mentioned hydrogen bond, as Tyr48 is located in the vicinity of the Asn52 residue. Alternatively, the protein−lipid interaction may be weakened by the additional negative charge in the phosphomimetic mutant. The cardiolipin interaction is intimately linked to the regulation of Cyt*c* peroxidase activity, which is normally inhibited in the presence of a hexacoordinated arrangement of the heme iron. As peroxidase activity requires a tyrosine radical (*29*), we hypothesized that mutation of one of the two tyrosine residues (48 and 67) located within 5 Å of the heme might have a profound effect. Our data, however, do not provide conclusive evidence of a role for Tyr48 in Cyt*c* peroxidase activity. The background peroxidase activity measured in the absence of inducing cardiolipin was significantly higher in the phosphomimetic mutant compared to wild type or the Tyr48Phe mutant. This observation may reflect an altered structural state of the Tyr48Glu mutant, being partially unfolded, allowing access of peroxide substrates to the heme. Interestingly, the background peroxidase activity of the Tyr48Glu variant was only induced by high concentrations of CL (50%, Figure 6B). In contrast, activities of both wild type and Tyr48Phe were several-fold induced at lower CL concentrations (20%), achieving much higher rates than the phosphomimetic mutant under these conditions. Whether this is a result of altered cardiolipin binding, as suggested by decreased affinity, or rather a change in the kinetics of the peroxidase reaction, has to be addressed in future studies. It can be concluded, however, that Tyr48 is not the only aromatic residue that would be indispensable for the peroxidase activity, as the Tyr48Phe mutant displayed comparable reaction rates and a similar mode of cardiolipin induction as wild-type Cyt*c*. Whether the decrease of cardiolipin binding and induction of peroxidase activity in Tyr48Glu Cyt*c* leads to inhibition of its release from mitochondria after apoptotic stimuli warrants future *in vivo* studies.

Arguably the most striking finding of the present study is the inability of the Tyr48Glu mutant to induce caspase-3 activation in cytosplasmic extracts. A substantial part of the Cyt*c* molecule is involved in the electrostatic interaction with Apaf-1, including "front face" lysine residues 7, 25, and 72, as well as the opposite surface segment centered around residues 39 and 62−65 (*43*), accounting for an exceptionally high affinity of binding (*19*). Lys72 is considered the most crucial residue for Apaf-1 binding; its trimethylation in yeast Cyt*c* yields an enzyme unable to initiate caspase activation, as further directly evidenced by the defect of apoptosome formation in Cyt*c* Lys72 mutants (*43*−*46*). However, Tyr48 is not located in the direct vicinity of the positively charged binding surfaces. Therefore, it seems unlikely that a negative charge introduced by the Tyr48Glu mutation would suffice to disrupt the electrostatic interaction of the two proteins. Whether the postulated flipping out of Tyr48 from the heme crevice upon its phosphorylation (*11*) or the Glu mutation causes a more substantial conformational change that interferes with Apaf-1 binding requires detailed structural studies. Other factors that influence apoptosome formation by Cyt*c* are its redox state (*47*) and nucleotide (ATP, dATP) binding (*48*, *49*). Concerning the redox state of Cyt*c*, it has been argued that its oxidized state is much more efficient in inducing apoptosis. This state of Cyt*c* in an apoptotic cell would be achieved after disruption of the outer mitochondrial membrane and mixing of the cytosolic and mitochondrial intermembrane compartments, making CcO freely available to oxidize the released Cyt*c* previously reduced by components of the cytosol (*47*). Our experiments have therefore been performed with oxidized enzymes. However, Cyt*c* was presumably reduced during the experiment after incubation with cytosolic extracts prepared from nonapoptotic cells (*50*), but they still efficiently induced caspase activity with the exception of the Tyr48Glu variant. It seems unlikely that the defect of induction of apoptosis by the phosphomimetic mutant can be attributed to a faster rate of reduction, since its redox potential is the lowest of the three enzyme variants, making it more difficult to reduce. The effect of nucleotides (ATP or dATP specifically) on apoptosome formation is biphasic. Low millimolar concentrations of ATP are required for assembly of the complex, while slightly higher concentrations (5−10 mM) completely inhibit it (*48*). The inhibition occurs through ATP interaction with Cyt*c*, since ATP and Apaf-1 compete for the positively charged lysine residues 7, 25, 39, and 72 on Cyt*c* (*48*). The interaction with ATP is unlikely to account for the observed inability of caspase activation by the Tyr48Glu mutant, as this residue is not positioned close to any of the three nucleotide binding sites of Cyt*c* (*48*).

The activity of Cyt*c* to induce apoptosis is generally regarded as separated from its function in electron transport, since the majority of Cyt*c* mutants that affect apoptosome assembly maintain normal respiration rates (*43*−*45*). Furthermore, replacement of the heme iron by zinc, resulting in Cyt*c* that is inactive in electron transport, allows initiation of the apoptotic cascade (*51*). In this regard, the effect of the phosphomimetic substitution is profound, because it partially inhibits electron transport and completely abolishes caspase-3 activation.

In summary, the Tyr48Glu mutant, mimicking our recently discovered *in vivo* phosphorylated Cyt*c* isolated from bovine liver, affected all functional aspects of the enzyme that we studied. Our findings therefore indicate the strategic position and role of Tyr48 in Cyt*c* and underscore the possibility that Tyr48 phosphorylation regulates multiple functions of Cyt*c* in cell life and cell death.

ACKNOWLEDGMENT

We thank Dr. Jeffrey W. Doan for suggestions on the manuscript and Dr. Lucy Waskell for helpful discussions.

SUPPORTING INFORMATION AVAILABLE

One figure as described in the text. This material is available free of charge via the Internet at http://pubs.acs.org.

REFERENCES

1. Li, K., Li, Y., Shelton, J. M., Richardson, J. A., Spencer, E., Chen, Z. J., Wang, X., and Williams, R. S. (2000) Cytochrome *c* deficiency causes embryonic lethality and attenuates stress-induced apoptosis. *Cell 101*, 389–399.
2. Morriss, G. M., and New, D. A. (1979) Effect of oxygen concentration on morphogenesis of cranial neural folds and neural crest in cultured rat embryos. *J. Embryol. Exp. Morphol. 54*, 17–35.
3. Kroemer, G., Dallaporta, B., and Resche-Rigon, M. (1998) The mitochondrial death/life regulator in apoptosis and necrosis. *Annu. Rev. Physiol. 60*, 619–642.
4. Skulachev, V. P. (1998) Cytochrome *c* in the apoptotic and antioxidant cascades. *FEBS Lett. 423*, 275–280.
5. Green, D. R. (2000) Apoptotic pathways: paper wraps stone blunts scissors. *Cell 102*, 1–4.
6. Kagan, V. E., Tyurina, Y. Y., Bayir, H., Chu, C. T., Kapralov, A. A., Vlasova II, Belikova, N. A., Tyurin, V. A., Amoscato, A., Epperly, M., Greenberger, J., Dekosky, S., Shvedova, A. A., and Jiang, J. (2006) The "pro-apoptotic genies" get out of mitochondria: oxidative lipidomics and redox activity of cytochrome *c*/cardiolipin complexes. *Chem. Biol. Interact. 163*, 15–28.
7. Pereverzev, M. O., Vygodina, T. V., Konstantinov, A. A., and Skulachev, V. P. (2003) Cytochrome *c*, an ideal antioxidant. *Biochem. Soc. Trans. 31*, 1312–1315.
8. Giorgio, M., Migliaccio, E., Orsini, F., Paolucci, D., Moroni, M., Contursi, C., Pelliccia, G., Luzi, L., Minucci, S., Marcaccio, M., Pinton, P., Rizzuto, R., Bernardi, P., Paolucci, F., and Pelicci, P. G. (2005) Electron transfer between cytochrome *c* and p66Shc generates reactive oxygen species that trigger mitochondrial apoptosis. *Cell 122*, 221–233.
9. Ferguson-Miller, S., Brautigan, D. L., and Margoliash, E. (1976) Correlation of the kinetics of electron transfer activity of various eukaryotic cytochromes *c* with binding to mitochondrial cytochrome *c* oxidase. *J. Biol. Chem. 251*, 1104–1115.
10. Lee, I., Salomon, A. R., Yu, K., Doan, J. W., Grossman, L. I., and Hüttemann, M. (2006) New prospects for an old enzyme: mammalian cytochrome *c* is tyrosine-phosphorylated in vivo. *Biochemistry 45*, 9121–9128.
11. Yu, H., Lee, I., Salomon, A. R., Yu, K., and Hüttemann, M. (2008) Mammalian liver cytochrome *c* is tyrosine-48 phosphorylated *in vivo*, inhibiting mitochondrial respiration. *Biochim. Biophys. Acta 1777*, 1066–1071.
12. Hüttemann, M., Lee, I., Samavati, L., Yu, H., and Doan, J. W. (2007) Regulation of mitochondrial oxidative phosphorylation through cell signaling. *Biochim. Biophys. Acta 1773*, 1701–1720.
13. Hüttemann, M., Lee, I., Pecinova, A., Pecina, P., Przyklenk, K., and Doan, J. W. (2008) Regulation of oxidative phosphorylation, the mitochondrial membrane potential, and their role in human disease. *J. Bioenerg. Biomembr. 40*, 445–456.
14. Bridges, A., Gruenke, L., Chang, Y. T., Vakser, I. A., Loew, G., and Waskell, L. (1998) Identification of the binding site on cytochrome P450 2B4 for cytochrome *b*5 and cytochrome P450 reductase. *J. Biol. Chem. 273*, 17036–17049.
15. Deep, S., Im, S. C., Zuiderweg, E. R., and Waskell, L. (2005) Characterization and calculation of a cytochrome *c*-cytochrome *b*5 complex using NMR data. *Biochemistry 44*, 10654–10668.
16. Miroux, B., and Walker, J. E. (1996) Over-production of proteins in *Escherichia coli*: mutant hosts that allow synthesis of some membrane proteins and globular proteins at high levels. *J. Mol. Biol. 260*, 289–298.
17. Cammack, R. (1995) Redox states and potentials, in Bioenergetics. A Practical Approach (Brown, G. C., and Cooper, C. E., Eds.) pp 85−109, Oxford University Press, Oxford.
18. Lee, I., Salomon, A. R., Yu, K., Samavati, L., Pecina, P., Pecinova, A., and Hüttemann, M. (2009) Isolation of regulatory-competent, phosphorylated cytochrome *c* oxidase. *Methods Enzymol. 457*, 193–210.
19. Slee, E. A., Harte, M. T., Kluck, R. M., Wolf, B. B., Casiano, C. A., Newmeyer, D. D., Wang, H. G., Reed, J. C., Nicholson, D. W., Alnemri, E. S., Green, D. R., and Martin, S. J. (1999) Ordering the cytochrome *c*-initiated caspase cascade: hierarchical activation of caspases-2, -3, -6, -7, -8, and -10 in a caspase-9-dependent manner. *J. Cell Biol. 144*, 281–292.
20. Borisenko, G. G., Kapralov, A. A., Tyurin, V. A., Maeda, A., Stoyanovsky, D. A., and Kagan, V. E. (2008) Molecular design of new inhibitors of peroxidase activity of cytochrome *c*/cardiolipin complexes: fluorescent oxadiazole-derivatized cardiolipin. *Biochemistry 47*, 13699–13710.
21. Folch, J., Lees, M., and Sloane Stanley, G. H. (1957) A simple method for the isolation and purification of total lipides from animal tissues. *J. Biol. Chem. 226*, 497–509.
22. Tyurin, V. A., Tyurina, Y. Y., Kochanek, P. M., Hamilton, R., DeKosky, S. T., Greenberger, J. S., Bayir, H., and Kagan, V. E. (2008) Oxidative lipidomics of programmed cell death. *Methods Enzymol. 442*, 375–393.
23. Chang, C. R., and Blackstone, C. (2007) Cyclic AMP-dependent protein kinase phosphorylation of Drp1 regulates its GTPase activity and mitochondrial morphology. *J. Biol. Chem. 282*, 21583–21587.
24. He, Y., Liu, J., Grossman, D., Durrant, D., Sweatman, T., Lothstein, L., Epand, R. F., Epand, R. M., and Lee, R. M. (2007) Phosphorylation of mitochondrial phospholipid scramblase 3 by protein kinase C-delta induces its activation and facilitates mitochondrial targeting of tBid. *J. Cell. Biochem. 101*, 1210–1221.
25. Kane, L. A., Youngman, M. J., Jensen, R. E., and Van Eyk, J. E. (2010) Phosphorylation of the F(1)F(o) ATP synthase beta subunit: functional and structural consequences assessed in a model system. *Circ. Res. 106*, 504–513.
26. Patel, C. N., Lind, M. C., and Pielak, G. J. (2001) Characterization of horse cytochrome *c* expressed in *Escherichia coli*. *Protein Expression Purif. 22*, 220–224.
27. Dickerson, R. E., and Timkovich, R. (1975) Cytochromes *c*, in The Enzymes (Boyer, P. D., Ed.) pp 397−547, Academic Press, New York.
28. Nicholls, D. G., and Ferguson, S. J. (2002) Bioenergetics, Vol. *3*, Academic Press, New York.
29. Kagan, V. E., Tyurin, V. A., Jiang, J., Tyurina, Y. Y., Ritow, V. B., Amoscato, A. A., Osipov, A. N., Belikova, N. A., Kapralov, A. A., Kini, V., Vlasova, I. I., Zhao, Q., Zou, M., Di, P., Svistunenko, D. A., Kurnikov, I. V., and Borisenko, G. G. (2005) Cytochrome *c* acts as a cardiolipin oxygenase required for release of proapoptotic factors. *Nat. Chem. Biol. 1*, 223–232.
30. Oellerich, S., Lecomte, S., Paternostre, M., Heimburg, T., and Hildebrandt, P. (2005) Peripheral and integral binding of cytochrome *c* to phospholipids vesicles. *J. Phys. Chem. B 108*, 3871–3878.
31. Sinibaldi, F., Fiorucci, L., Patriarca, A., Lauceri, R., Ferri, T., Coletta, M., and Santucci, R. (2008) Insights into cytochrome *c*-cardiolipin interaction. Role played by ionic strength. *Biochemistry 47*, 6928–6935.
32. Borisenko, G. G., Iverson, S. L., Ahlberg, S., Kagan, V. E., and Fadeel, B. (2004) Milk fat globule epidermal growth factor 8 (MFG-E8) binds to oxidized phosphatidylserine: implications for macrophage clearance of apoptotic cells. *Cell Death Differ. 11*, 943–945.
33. Belikova, N. A., Vladimirov, Y. A., Osipov, A. N., Kapralov, A. A., Tyurin, V. A., Potapovich, M. V., Basova, L. V., Peterson, J., Kurnikov, I. V., and Kagan, V. E. (2006) Peroxidase activity and structural transitions of cytochrome *c* bound to cardiolipin-containing membranes. *Biochemistry 45*, 4998–5009.
34. Sinibaldi, F., Howes, B. D., Piro, M. C., Polticelli, F., Bombelli, C., Ferri, T., Coletta, M., Smulevich, G., and Santucci, R. (2010) Extended cardiolipin anchorage to cytochrome *c*: a model for protein-mitochondrial membrane binding. *J. Biol. Inorg. Chem. 15*, 689–700.
35. Tyurina, Y. Y., Tyurin, V. A., Epperly, M. W., Greenberger, J. S., and Kagan, V. E. (2008) Oxidative lipidomics of gamma-irradiation-induced intestinal injury. *Free Radical Biol. Med. 44*, 299–314.
36. Gorbenko, G. P., Molotkovsky, J. G., and Kinnunen, P. K. (2006) Cytochrome *c* interaction with cardiolipin/phosphatidylcholine model membranes: effect of cardiolipin protonation. *Biophys. J. 90*, 4093–4103.

37. Kalanxhi, E., and Wallace, C. J. (2007) Cytochrome *c* impaled: investigation of the extended lipid anchorage of a soluble protein to mitochondrial membrane models. *Biochem. J. 407*, 179–187.
38. Belikova, N. A., Tyurina, Y. Y., Borisenko, G., Tyurin, V., Samhan Arias, A. K., Yanamala, N., Furtmuller, P. G., Klein-Seetharaman, J., Obinger, C., and Kagan, V. E. (2009) Heterolytic reduction of fatty acid hydroperoxides by cytochrome *c*/cardiolipin complexes: antioxidant function in mitochondria. *J. Am. Chem. Soc. 131*, 11288–11289.
39. Kagan, V. E., Bayir, H. A., Belikova, N. A., Kapralov, O., Tyurina, Y. Y., Tyurin, V. A., Jiang, J., Stoyanovsky, D. A., Wipf, P., Kochanek, P. M., Greenberger, J. S., Pitt, B., Shvedova, A. A., and Borisenko, G. (2009) Cytochrome *c*/cardiolipin relations in mitochondria: a kiss of death. *Free Radical Biol. Med. 46*, 1439–1453.
40. Rodriguez-Roldan, V., Garcia-Heredia, J. M., Navarro, J. A., Rosa, M. A., and Hervas, M. (2008) Effect of nitration on the physicochemical and kinetic features of wild-type and monotyrosine mutants of human respiratory cytochrome *c*. *Biochemistry 47*, 12371–12379.
41. Korshunov, S. S., Krasnikov, B. F., Pereverzev, M. O., and Skulachev, V. P. (1999) The antioxidant functions of cytochrome *c*. *FEBS Lett. 462*, 192–198.
42. Bayir, H., Fadeel, B., Palladino, M. J., Witasp, E., Kurnikov, I. V., Tyurina, Y. Y., Tyurin, V. A., Amoscato, A. A., Jiang, J., Kochanek, P. M., DeKosky, S. T., Greenberger, J. S., Shvedova, A. A., and Kagan, V. E. (2006) Apoptotic interactions of cytochrome *c*: redox flirting with anionic phospholipids within and outside of mitochondria. *Biochim. Biophys. Acta 1757*, 648–659.
43. Yu, T., Wang, X., Purring-Koch, C., Wei, Y., and McLendon, G. L. (2001) A mutational epitope for cytochrome *c* binding to the apoptosis protease activation factor-1. *J. Biol. Chem. 276*, 13034–13038.
44. Abdullaev, Z., Bodrova, M. E., Chernyak, B. V., Dolgikh, D. A., Kluck, R. M., Pereverzev, M. O., Arseniev, A. S., Efremov, R. G., Kirpichnikov, M. P., Mokhova, E. N., Newmeyer, D. D., Roder, H., and Skulachev, V. P. (2002) A cytochrome *c* mutant with high electron transfer and antioxidant activities but devoid of apoptogenic effect. *Biochem. J. 362*, 749–754.
45. Hao, Z., Duncan, G. S., Chang, C. C., Elia, A., Fang, M., Wakeham, A., Okada, H., Calzascia, T., Jang, Y., You-Ten, A., Yeh, W. C., Ohashi, P., Wang, X., and Mak, T. W. (2005) Specific ablation of the apoptotic functions of cytochrome *c* reveals a differential requirement for cytochrome *c* and Apaf-1 in apoptosis. *Cell 121*, 579–591.
46. Sharonov, G. V., Feofanov, A. V., Bocharova, O. V., Astapova, M. V., Dedukhova, V. I., Chernyak, B. V., Dolgikh, D. A., Arseniev, A. S., Skulachev, V. P., and Kirpichnikov, M. P. (2005) Comparative analysis of proapoptotic activity of cytochrome *c* mutants in living cells. *Apoptosis 10*, 797–808.
47. Brown, G. C., and Borutaite, V. (2008) Regulation of apoptosis by the redox state of cytochrome *c*. *Biochim. Biophys. Acta 1777*, 877–881.
48. Patriarca, A., Eliseo, T., Sinibaldi, F., Piro, M. C., Melis, R., Paci, M., Cicero, D. O., Polticelli, F., Santucci, R., and Fiorucci, L. (2009) ATP acts as a regulatory effector in modulating structural transitions of cytochrome *c*: implications for apoptotic activity. *Biochemistry 48*, 3279–3287.
49. Purring-Koch, C., and McLendon, G. (2000) Cytochrome *c* binding to Apaf-1: the effects of dATP and ionic strength. *Proc. Natl. Acad. Sci. U.S.A. 97*, 11928–11931.
50. Hampton, M. B., Zhivotovsky, B., Slater, A. F., Burgess, D. H., and Orrenius, S. (1998) Importance of the redox state of cytochrome *c* during caspase activation in cytosolic extracts. *Biochem. J. 329* (Part 1), 95–99.
51. Kluck, R. M., Martin, S. J., Hoffman, B. M., Zhou, J. S., Green, D. R., and Newmeyer, D. D. (1997) Cytochrome *c* activation of CPP32-like proteolysis plays a critical role in a *Xenopus* cell-free apoptosis system. *EMBO J. 16*, 4639–4649.